AGU PUBLICATIONS

Geophysical Research Letters

RESEARCH LETTER
10.1002/2017GL072588

Key Points:
- We propose a simple theory using the framework of Zebiak-Cane ocean model for insights into the dynamics of the upwelling annual cycle
- The annual upwelling can be decomposed into two parts: one impacted by locally Ekman pumping and the other by remotely ocean waves
- In the equatorial Atlantic, the annual upwelling is dominated by Ekman pumping in the west, whereas in the east it is owing to wave effects

Supporting Information:
- Supporting Information S1

Correspondence to:
F.-F. Jin,
jff@hawaii.edu

Citation:
Wang, L.-C., F.-F. Jin, C.-R. Wu, and H.-H. Hsu (2017), Dynamics of upwelling annual cycle in the equatorial Atlantic Ocean, *Geophys. Res. Lett.*, *44*, 3737–3743, doi:10.1002/2017GL072588.

Received 12 JAN 2017
Accepted 27 FEB 2017
Accepted article online 2 MAR 2017
Published online 19 APR 2017

Dynamics of upwelling annual cycle in the equatorial Atlantic Ocean

Li-Chiao Wang[1,2], Fei-Fei Jin[3], Chau-Ron Wu[1,2], and Huang-Hsiung Hsu[2]

[1]Department of Earth Sciences, National Taiwan Normal University, Taipei, Taiwan, [2]Research Center for Environmental Change, Academia Sinica, Taipei, Taiwan, [3]Department of Atmospheric Sciences, University of Hawai'i at Mānoa, Honolulu, Hawaii, USA

Abstract The annual upwelling is an important component of the equatorial Atlantic annual cycle. A simple theory is proposed using the framework of Zebiak-Cane (ZC) ocean model for insights into the dynamics of the upwelling annual cycle. It is demonstrated that in the Atlantic equatorial region this upwelling is dominated by Ekman processing in the west, whereas in the east it is primarily owing to shoaling and deepening of the thermocline resulting from equatorial mass meridional recharge/discharge and zonal redistribution processes associated with wind-driven equatorial ocean waves. This wind-driven wave upwelling plays an important role in the development of the annual cycle in the sea surface temperature of the cold tongue in the eastern equatorial Atlantic.

1. Introduction

Equatorial upwelling plays a vitally important role not only in the cold tongue development but also the variations of oceanic productivity. For instance, the cold tongue sea surface temperature (SST) reaches its minimum in the summer, which tends to follow right after the peak upwelling in the earlier summer, clearly indicating that important dynamic cooling effect in dictating the phasing of the equatorial cold tongue SST annual cycle [*Clement et al*., 1997; *An et al*., 2012]. Moreover, the enhancing or weakening of equatorial upwelling is closely related to nutrients concentration and primary productivity [*Dandonneau et al*., 2004].

A number of studies have been directed to survey the spatial distributions and temporal evolutions of SST, thermocline displacement, trade winds, and horizontal ocean circulations in tropical Atlantic and to investigate the dynamics of interannual variability [*Zebiak*, 1993; *Keenlyside and Latif*, 2007] and seasonal cycle [*Merle et al*., 1980; *Li and Philander*, 1997; *Ding et al*., 2009]. Considerable efforts have also been made on analyzing the seasonal upwelling in the equatorial Atlantic. Most studies suggested that the equatorial upwelling is largely attributable to Ekman pumping driven by local winds [*Weingartner and Weisberg*, 1991; *Hagos and Cook*, 2009; *Li and Philander*, 1997]. A number of studies pointed out the importance of equatorial easterlies and cross-equatorial southerlies for the seasonal cooling by inducing local upwelling and raising the thermocline in the east [*Okumura and Xie*, 2004; *Richter and Xie*, 2008; *Caniaux et al*., 2011]. A recent study suggested that the equatorial upwelling is mainly resulted from the turbulent momentum flux and the imbalance between circulation and pressure fields [*Giordani and Caniaux*, 2011]. However, limited attention has been made about the basic dynamics of the equatorial Atlantic upwelling annual cycle despite its essential role in the equatorial Atlantic climatic annual cycle. In this work, we propose a simple theory based on the framework of the model by *Zebiak and Cane* [1987, hereafter denoted as ZC87] to demonstrate that the equatorial upwelling is controlled by both the locally wind-driven Ekman process and remotely forced wave effect.

Section 2 describes the data sets used in this work, sections 3 and 4 provide a simple formulation of the equatorial upwelling and its validation as well as discussions on the role of the recharge/discharge process in its contribution to upwelling, and finally, section 5 provides the conclusion.

2. Data

The observational data including vertical velocity, SST, wind stresses, and 20°C isotherm depth which represents the thermocline depth are obtained from the European Centre for Medium-Range Weather Forecasts (ECMWF) operational ocean analysis/reanalysis system (ORA-S3, available at http://apdrc.soest.hawaii.edu/data/data.php and *Balmaseda et al*. [2008], for the period 1959–2009). The fine equatorial resolution of ORA-S3 is important in analyzing the ocean-atmosphere dynamics in tropical Pacific [*Zhai and Hu*, 2013; *Jin*

et al., 2014]. It is also frequently used to resolve the prominent Atlantic variability in northern [*Balmaseda et al*., 2007; *Munoz et al*., 2011] and equatorial [*Nnamchi et al*., 2015, 2016] area and thus will be also utilized for this study. The annual cycles are defined in this work as the anomalies with respect to the climate annual mean of the entire data period.

3. A Simple Theory of the Equatorial Upwelling

3.1. Formulation

Using the ocean component of the ZC87 model, we can derive the following formulation for the equatorial upwelling:

$$w = w_e \cdot [1 - R(x)] + w_h \cdot R(x) \tag{1}$$

$$R(x) = H_1/H(x) = 50/H(x) = 1 \quad \text{if} \quad H(x) < 50 \tag{2}$$

This equatorial upwelling consists a linear combination of two parts, the Ekman upwelling and wave upwelling, denoted as W_e and W_h, respectively. The wave upwelling can be expressed as $-\partial h/\partial t$ (h denotes the thermocline depth), namely, the negative thermocline tendency. Here H and H_1 refer to the climate mean thermocline depth and a constant mixed layer depth. This formulation for upwelling is essentially the same as that of ZC87 except that the zonal variations in the climate mean of thermocline depth is taken into consideration such that the weighting function $R(x)$ depends on longitude as well (detailed derivations are given in supporting information A).

3.2. Validation

In order to obtain theoretical equatorial vertical velocity as formulated in equation (1), we need to use (1) observed surface wind stress to calculate the Ekman upwelling W_e following the formulation of ZC87 (also see supporting information A), (2) observed thermocline depth to calculate W_h, and (3) observed climate mean depth of thermocline $H(x)$ to calculate $R(x)$. We then compare this estimated W directly with the observational vertical velocity at 50 m from ECMWF reanalysis data (Figure 1). The observed equatorial Atlantic upwelling annual cycle is dominated by a strong annual harmonic component in the west and an evident semiannual harmonic component in the east (Figure 1a). Both features are captured by the theoretical estimated W (Figure 1b), and the time-longitude evolution pattern correlation (simply referred to as pattern correlation hereafter) between the observed and theoretical estimated vertical velocity reaches 0.82, indicating that the simple formulation of equation (1) is reasonably successful.

With our simple formulation, we now can further examine the contributions to the 50 m vertical velocity from the Ekman upwelling (Figure 1c) and wave upwelling. The Ekman upwelling is dominated in the western Atlantic with a clear prevailing annual harmonic component with its phasing similar to the observed upwelling. In the east, however, the Ekman upwelling is much weaker. The pattern correlation between the observed vertical velocity in Figure 1a and the derived Ekman upwelling is about 0.53, indicating clearly that it alone is not adequate to represent the equatorial upwelling annual cycle in the Atlantic. By contrast, the wave upwelling (Figure 1d) displays a strong semiannual signal in the eastern Atlantic with similar phases to the observed upwelling. Nevertheless, the pattern correlation between the observed vertical velocity and the wave upwelling is about 0.56, also indicating that it alone is not adequate to represent the equatorial upwelling annual cycle in the Atlantic. It should be noted that the contributions of Ekman and wave upwellings to the total vertical velocity are further weighted by functions $1 - R(x)$ and $R(x)$ respectively, which weights heavily on the Ekman upwelling in the west and wave upwelling in the east. As a result, this weighted combination derived from the ZC87 model is thus naturally in the best way to capture contributions from the Ekman upwelling in the west and wave upwelling in the east, respectively.

The different contributions from the Ekman upwelling in the west and wave upwelling in the east are further delineated in Figures 1e and 1f. In the west, the Ekman and wave effects are both important. The Ekman upwelling attains its maximum 1 month before the observed upwelling peaks and serves as a main contributor to the development of the observed peak upwelling. The wave upwelling tends to contribute negatively and thus to cancel a part of the Ekman upwelling so that the combination is in a better agreement with the observation (Figure 1e). By contrast, in the eastern equatorial Atlantic, the wave upwelling serves as a

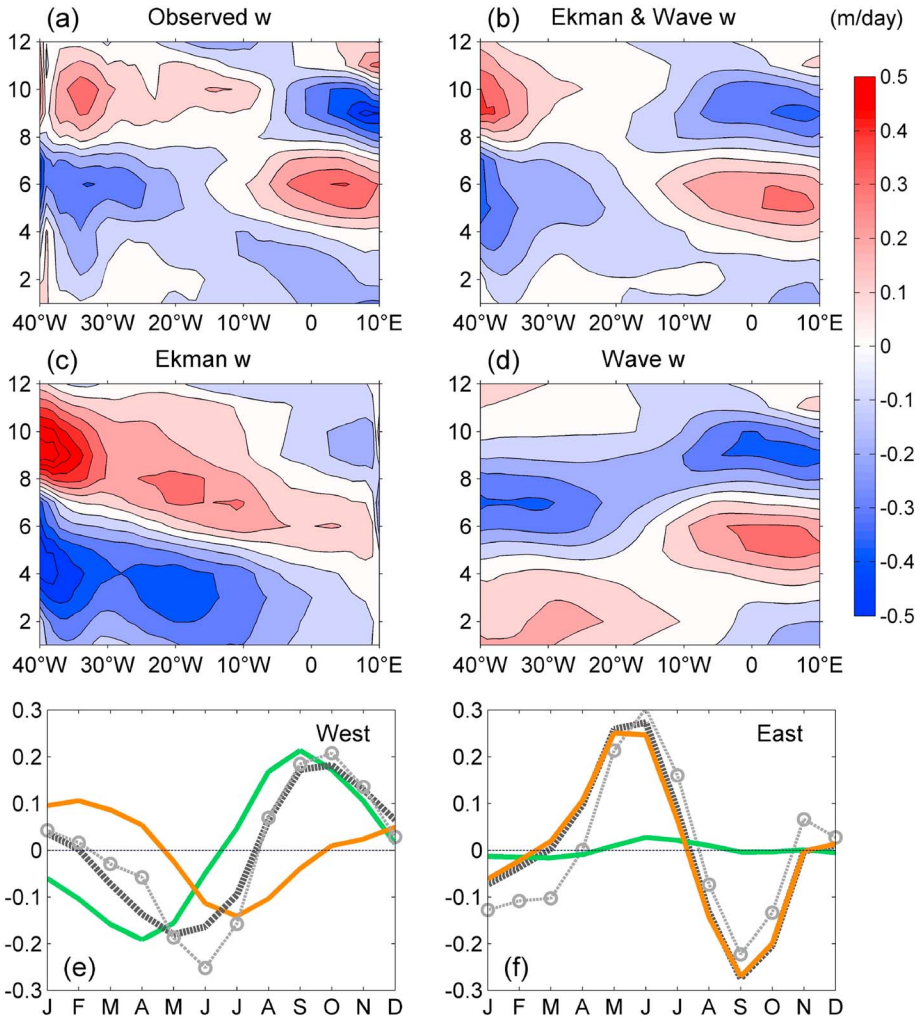

Figure 1. The annual cycles of the (a) observed (b) theoretical (c) Ekman and (d) wave upwelling in the equatorial Atlantic (averaged in 3°N–3°S). The equatorial Atlantic annual cycles of the observed (gray circle), theoretical (dashed black), contributions from the Ekman (green), and wave (orange) upwellings over the (e) western (3°N–3°S, 40°W–20°W) and (f) eastern (3°N–3°S, 10°W–10°E) regions are further contrasted (units: m/d).

dominant contributor to the observed upwelling annual cycle, whereas the Ekman upwelling contributes very little (Figure 1f).

4. Dynamics of Wave Upwelling

4.1. Shallow Water Modeling

Since Ekman upwelling is simply related to the local wind stress forcing with a very simple formulation, we now focus on our understanding of the equatorial upwelling dynamics on the wave component. To discern the dynamics of wave upwelling, a shallow-water model (hereafter denoted as SWM) [*Mcgregor et al*., 2007] forced by observed wind stresses is used to simulate the wave upwelling. To make the model applicable to the tropical Atlantic basin, we reduce the gravity wave speed by multiplying a factor of 0.6 so that the model-simulated thermocline depth is comparable in amplitude with the observation. As noted by a number of studies [e.g., *Bunge and Clarke*, 2009; *Ding et al*., 2009], we also find SWM successfully captures the annual evolution of the equatorial thermocline (Figures 2a and 2b, shadings). The pattern correlation between observational and modeled thermocline depth is 0.87. Our emphasis here, however, is the remarkable agreement of the simulated wave upwelling with the observed wave upwelling as estimated by observed thermocline tendency (Figures 2a and 2b, contours), attaining pattern correlation also as high as 0.87.

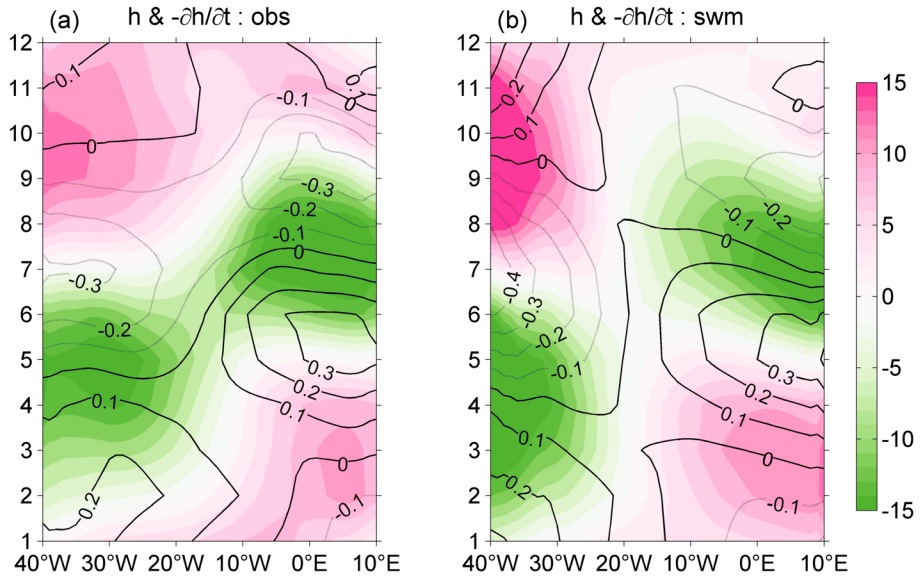

Figure 2. The equatorial Atlantic annual cycles (averaged in 3°N–3°S) of the thermocline (shadings, units: m) and the observed wave upwelling estimated by thermocline tendencies (contours, units: m/d) in (a) observation and (b) SWM simulations.

4.2. Meridional Recharge/Discharge and Zonal Mass Redistribution Processes

The wave upwelling in the eastern Atlantic could be further examined through the approach first mentioned in *Jin* [1996] and thereafter fully developed by *Jin* [1997] in his simple formulation for understanding the heat content dynamics associated with El Niño Southern–Oscillation (ENSO) recharge oscillator. Wave upwelling in our paper refers to the upwelling/downwelling due to thermocline depth tendency. As in *Jin* [1997], we may understand the evolution of the equatorial thermocline in terms of the fast buildup of zonal contrast of thermocline depth through mass redistribution in zonal direction by the equatorial Kelvin and Rossby waves and slow meridional recharge/discharge to control the equatorial zonal mean of the thermocline depth. This allows us to express the eastern thermocline depth (tendency) in terms of central basin wind stress (tendency) and zonal mean thermocline (tendency) (see detailed derivations in supporting information B), which shall give us further insights into the dynamics of wave upwelling.

For simplicity, we define western, central, eastern equatorial Atlantic regions as (3°N–3°S, 40°W–20°W), (3°N–3°S, 30°W–0°E), and (3°N–3°S, 10°W–10°E), respectively. Indeed, the zonal contrast of thermocline is in quasi-equilibrium with the central basin wind stress (Figure 3a), indicating that this zonal contrast is achieved by relatively fast process of wave adjustment. Further, the eastern basin thermocline (tendency) can be neatly expressed as the combination of zonal mean thermocline depth (tendency) and the central basin wind stress (tendency) (Figure 3b). We here focus on this balance in terms of tendencies, because we focus on the wave upwelling in the eastern basin. The correlation between estimated upwelling by this simple balance equation and the observed/SWM-simulated eastern wave upwelling is as high as 0.98/0.99. Thus, eastern wave upwelling can be understood in terms of shoaling and deepening of thermocline of both zonal mean and zonal contrast. The former is associated with relatively slow meridional heat content discharge and thus about out of phase with the zonal wind forcing, whereas the latter is in quasi-balance with the wind forcing.

As in the ENSO recharge oscillator, here the annual cycles in the zonal contrast and zonal mean of the equatorial thermocline are in 90° phase quadrature, which is vividly illustrated in Figure 3c. The same holds true for their tendencies (Figure 3d). Thus, the fundamental process of ocean heat recharge/discharge for the ENSO recharge oscillator is clearly at work and plays an important role in the eastern Atlantic upwelling. To further quantitatively examine the contributions of the recharge/discharge relative to the zonal thermocline contrast, Figure 3e displays the observed wave upwelling (black thick line), together with the two parts associated with upwelling owing to zonal thermocline contrast tendency expressed in terms of central basin wind stress tendency (green line) and zonal mean thermocline depth tendency (red line), respectively. The wave

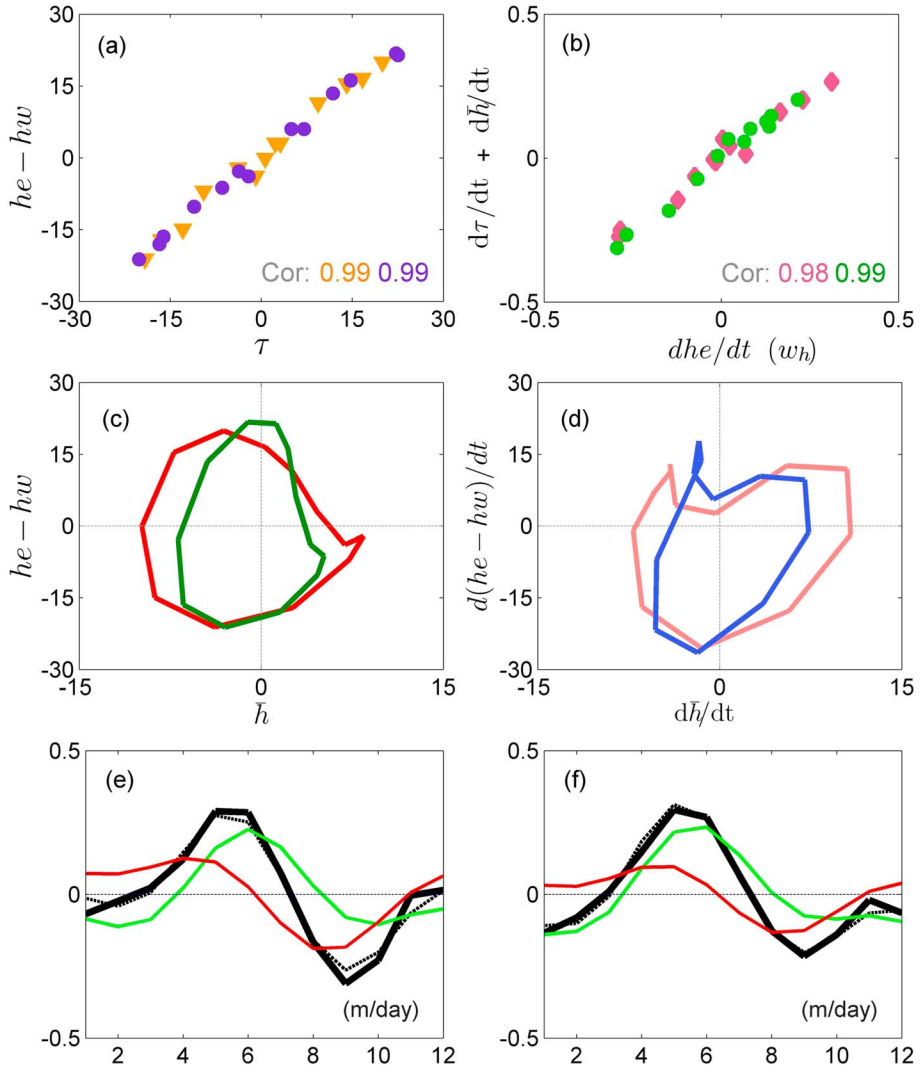

Figure 3. The relationship (a) between the central basin wind stress and the zonal contrast of thermocline in observation (triangles) and SWM simulations (circles), (b) between the wave upwelling estimated by eastern basin thermocline tendency and the combination of zonal mean thermocline tendency together with the central basin wind stress tendency in observation (diamonds) and SWM simulations (circles), (c) between the zonal contrast and zonal mean of the equatorial thermocline in observation (red) and SWM simulations (green), and (d) between the tendencies of the zonal contrast and zonal mean of the equatorial thermocline in observation (pink) and SWM simulations (blue). (e, f) Illustration of the observed (black thick lines) and the estimated (black dash lines) wave upwelling together with two parts: one owing to the mean thermocline depth tendency (red) and the other associated with the central basin wind stress tendency (green) in observation and SWM simulations, respectively (units: m/d).

upwelling estimated by these two parts (black dash line) perfectly matches the observed one. It is evident that both processes contribute to the wave upwelling substantially with the recharge/discharge process playing a crucial role in the observed wave upwelling and consequently the total eastern Atlantic upwelling annual cycle. Furthermore, the two contributing processes identified in the observation data are nicely simulated in SWM (Figure 3f), indicating the robustness of the simple dynamics of wave upwelling.

4.3. Annual Cycles of the Equatorial Upwelling and SST

To discern the role of this dynamic process of the wave upwelling in equatorial Atlantic annual cycle, we pair the equatorial upwelling and SST annual cycle all together in Figure 4. The SST cold peak at the end of July in the eastern equatorial Atlantic is accompanied by an earlier strong upwelling peak around June and a strong downwelling in September. Thus, the strong development and rapid decline of the cold phase of the SST

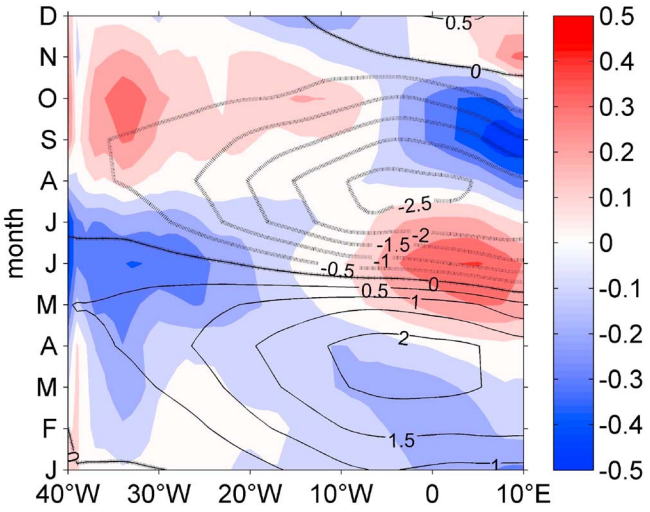

Figure 4. The annual cycles of upwelling (shading, units: m/d) and SST (contour, units: degrees) in the equatorial Atlantic (averaged in 3°N–3°S).

annual cycle and the concurrent rapid transition from dynamic wave upwelling to downwelling in only about 3 months apart suggest that Atlantic cold tongue SST annual cycle is heavily affected by wave upwelling, implying that coupled wave dynamics may play an important role in the Atlantic annual cycle.

5. Conclusions

Atlantic equatorial upwelling and its annual cycle are key dynamic features in tropical climate system and marine ecosystem. A number of processes have been identified to play contributing roles in the upwelling annual cycle [e.g., *Weingartner and Weisberg*, 1991; *Li and Philander*, 1997; *Okumura and Xie*, 2004; *Richter and Xie*, 2008; *Caniaux et al*., 2011; *Giordani and Caniaux*, 2011]. Nevertheless, the basic dynamics of the equatorial Atlantic upwelling annual cycle has yet to be succinctly delineated. In this work, we propose a simple theory based on ZC87 model's framework to delineate the essential dynamics controlling the Atlantic equatorial upwelling annual cycle. This later can be understood in terms of locally wind-driven Ekman pumping and remotely wind-driven wave upwelling associated with thermocline shoaling and deepening. We demonstrate clearly that the Ekman upwelling, which was generally thought to be the main source of equatorial upwelling, is in fact only a fraction of the total upwelling. It mainly dominates the upwelling in the western equatorial Atlantic, whereas the eastern equatorial Atlantic is dominated by wave upwelling. We further demonstrate that wave upwelling in the eastern Atlantic can be divided into two parts: a part associated with upwelling owing to zonal thermocline contrast tendency expressed in terms of central basin wind stress tendency, and the other part associated with upwelling in terms of zonal mean thermocline depth tendency which is related to the same recharge/discharge dynamic process known to be important for ENSO recharge oscillator. Our studies call attention to reexamine the basic dynamics of Atlantic equatorial cold tongue SST annual cycle and its internal variability on one hand and also provide a useful tool to understand the equatorial Atlantic and Pacific upwelling and its simulations in climate models. Some further results on these topics will be discussed in other forthcoming papers.

Acknowledgments
The authors would like to thank the Editor and the anonymous reviewers for their careful review of the manuscript and detailed suggestions to improve the manuscript. This study was jointly supported by the Ministry of Science and Technology (MOST), Taiwan, under grant 100-2119-M-001-029-MY5, U.S. National Science Foundation (NSF) grant AGS-1406601, and U.S. Department of Energy grant DE-SC0005110. CRW was additionally supported by 105-2119-M-003-003 and 104-2611-M-003-002-MY3. The data used in this study is listed in section 2 at http://apdrc.soest.hawaii.edu/data/data.php.

References

An, S. I., J. W. Kim, S. H. Im, B. M. Kim, and J. H. Park (2012), Recent and future sea surface temperature trends in tropical Pacific warm pool and cold tongue regions, *Clim. Dyn.*, *39*(6), 1373–1383, doi:10.1007/s00382-011-1129-7.

Balmaseda, M., A. Vidard, and D. L. T. Anderson (2008), The ECMWF Ocean Analysis System: ORA-S3, *Mon. Weather Rev.*, *136*, 3018–3034, doi:10.1175/2008MWR2433.1.

Balmaseda, M. A., G. C. Smith, K. Haines, D. Anderson, T. N. Palmer, and A. Vidard (2007), Historical reconstruction of the Atlantic Meridional Overturning Circulation from the ECMWF operational ocean reanalysis, *Geophys. Res. Lett.*, *34*, L23615, doi:10.1029/2007GL031645.

Bunge, L., and A. J. Clarke (2009), Seasonal propagation of sea level along the equator in the Atlantic, *J. Phys. Oceanogr.*, *39*(4), 1069–1074, doi:10.1175/2008JPO4003.1.

Caniaux, G., H. Giordani, J. L. Redelsperger, F. Guichard, E. Key, and M. Wade (2011), Coupling between the Atlantic cold tongue and the West African monsoon in boreal spring and summer, *J. Geophys. Res.*, *116*, C04003, doi:10.1029/2010JC006570.

Clement, A. C., R. Seager, M. Cane, and S. E. Zebiak (1997), An ocean dynamical thermostat, *Oceanogr. Lit. Rev.*, *6*(44), 556, doi:10.1175/1520-0442(1996)009<2190:AODT>2.0.CO;2.

Dandonneau, Y., P. Y. Deschamps, J. M. Nicolas, H. Loisel, J. Blanchot, Y. Montel, F. Thieuleux, and G. Bécu (2004), Seasonal and interannual variability of ocean color and composition of phytoplankton communities in the North Atlantic, equatorial Pacific and South Pacific, *Deep Sea Res., Part II*, *51*(1), 303–318, doi:10.1016/j.dsr2.2003.07.018.

Ding, H., N. S. Keenlyside, and M. Latif (2009), Seasonal cycle in the upper equatorial Atlantic Ocean, *J. Geophys. Res.*, *114*, C09016, doi:10.1029/2009JC005418.

Giordani, H., and G. Caniaux (2011), Diagnosing vertical motion in the Equatorial Atlantic, *Ocean Dyn.*, *61*(12), 1995–2018, doi:10.1007/s10236-011-0467-7.

Hagos, S. M., and K. H. Cook (2009), Development of a coupled regional model and its application to the study of interactions between the West African monsoon and the eastern tropical Atlantic Ocean, *J. Clim.*, *22*(10), 2591–2604, doi:10.1175/2008JCLI2466.1.
Jin, F. F., J. Boucharel, and I. I. Lin (2014), Eastern Pacific tropical cyclones intensified by El Niño delivery of subsurface ocean heat, *Nature*, *516*(7529), 82–85.
Jin, F.-F. (1996), Tropical ocean-atmosphere interaction, the Pacific cold tongue, and the El Niño-Southern Oscillation, *Science*, *274*(5284), 76.
Jin, F.-F. (1997), An equatorial ocean recharge paradigm for ENSO. Part I: Conceptual model, *J. Atmos. Sci.*, *54*(7), 811–829, doi:10.1175/1520-0469(1997)054<0811:AEORPF>2.0.CO;2.
Keenlyside, N. S., and M. Latif (2007), Understanding equatorial Atlantic interannual variability, *J. Clim.*, *20*(1), 131–142.
Li, T., and S. G. H. Philander (1997), On the seasonal cycle of the equatorial Atlantic Ocean, *J. Clim.*, *10*, 813–817, doi:10.1175/1520-0442(1997)010<0813:OTSCOT>2.0.CO;2.
McGregor, S., N. J. Holbrook, and S. B. Power (2007), Interdecadal sea surface temperature variability in the equatorial Pacific Ocean. Part I: The role of off-equatorial wind stresses and oceanic Rossby waves, *J. Clim.*, *20*(11), 2643–2658, doi:10.1175/JCLI4145.1.
Merle, J., M. Fieux, and P. Hisard (1980), Annual signal and interannual anomalies of sea surface temperature in the eastern equatorial Atlantic Ocean, *Deep Sea Res.*, *26*, 77–102.
Munoz, E., B. Kirtman, and W. Weijer (2011), Varied representation of the Atlantic meridional overturning across multidecadal ocean reanalyses, *Deep Sea Res., Part II*, *58*(17), 1848–1857.
Nnamchi, H. C., J. Li, F. Kucharski, I. S. Kang, N. S. Keenlyside, P. Chang, and R. Farneti (2015), Thermodynamic controls of the Atlantic Niño, *Nat. Commun.*, *6*, doi:10.1038/ncomms9895.
Nnamchi, H. C., J. Li, F. Kucharski, I. S. Kang, N. S. Keenlyside, P. Chang, and R. Farneti (2016), An Equatorial–Extratropical Dipole Structure of the Atlantic Niño, *J. Clim.*, *29*(20), 7295–7311.
Okumura, Y., and S. P. Xie (2004), Interaction of the Atlantic equatorial cold tongue and the African monsoon, *J. Clim.*, *17*(18), 3589–3602.
Richter, I., and S. P. Xie (2008), On the origin of equatorial Atlantic biases in coupled general circulation models, *Clim. Dyn.*, *31*(5), 587–598, doi:10.1007/s00382-008-0364-z.
Weingartner, T. J., and R. H. Weisberg (1991), On the annual cycle of equatorial upwelling in the central Atlantic Ocean, *J. Phys. Oceanogr.*, *21*, 68–82, doi:10.1175/1520-0485(1991)021<0068:OTACOE>2.0.CO;2.
Zebiak, S. E. (1993), Air–sea interaction in the equatorial Atlantic region, *J. Clim.*, *6*(8), 1567–1586.
Zebiak, S. E., and M. A. Cane (1987), A model El Niño–Southern Oscillation, *Mon. Weather Rev.*, *115*(10), 2262–2278, doi:10.1175/1520-0493(1987)115<2262:AMENO>2.0.CO;2.
Zhai, F., and D. Hu (2013), Revisit the interannual variability of the North Equatorial Current transport with ECMWF ORA-S3, *J. Geophys. Res. Oceans*, *118*, 1349–1366, doi:10.1002/jgrc.20093.